Population's Exposures to Pollens in Different Climate Regions in United States

From: Kun Mei

To: Dr. Panos G. Georgopoulos ,Yong Zhang

Date: Dec 6, 2013

1 Abstract

its distributions exhibit considerable variability in space and time. We can display both the temporal and spatial distributions based on either the mechanism models or statistical models using Matlab. Then we use Monte-Carlo method to predict the exposure effect of the pollen in different areas finally we using OAT sensitivity analysis to analyze the sensitivity of those physical parameters related to route of the exposure of pollens to human

2 Introduction

Airborne allergenic such as pollens, which has been found to act synergistically with common air pollutants, such as ozone, will cause allergic airway disease (AAD).and related rising public health costs(Lamb, Ratner et al. 2006, Singh, Axelrod et al. 2010). One third of the US population are impacted by allergic diseases, including asthma, hay fever, rhinitis, and atopic dermatitis(Bielory, Lyons et al. 2012) These allergic diseases can be potentially triggered and exacerbated by allergenic pollen, such as birch and oak, under climate change scenarios(Shea, Truckner et al.

2008). Synergism of pollen with other common atmospheric pollutants under conditions of climate change has been identified and has enhanced the severity of AAD(Adhikari, Reponen et al. 2006).

Pollen Exposure to Human can occur via inhalation, dermal contact as well as unintentional ingestion.

3 Background Information

3.1 Pollen and allergy

Rhinitis, conjunctivitis and asthma are often considered as the typical clinical pictures of allergy to pollens and they often occur in the same patient simultaneously during the pollen season(Sofiev, Belmonte et al. 2013).Asthma is a chronic in flammatory disease of the airways characterized by recurrent episodes of wheezing, breathlessness, chest tightness and coughing (Bateman, Hurd et al. 2008).Exposure to allergens represents a key factor among environmental determinants of asthma, which also include air pollution(Eder, Ege et al. 2006). Allergic rhinitis is clinically defined as a symptomatic disorder of the nose induced by an IgE-mediated in flammation after allergen exposure of the membranes lining the nose. Symptoms of rhinitis include rhinorrhea, nasal obstruction, nasal itching and sneezing which are reversible spontaneously or (Brożek, Bousquet et al. 2010)under treatment .Pathophysiological and clinical studies have strongly suggested a relationship between rhinitis and asthma. However, epidemiology provides the most convincing data, showing that the prevalence of asthma in patients with rhinitis varies from 10 to 40 % depe\ding on the study(Sofiev, Belmonte et al. 2013). Moreover,

allergic rhinitis is correlated to, and constitutes a risk factor for, the occurrence of asthma. Taken together, these data have led to the concept that upper and lower airways may be considered as a unique entity influenced by a common, evolving in flammatory process. (Passalacqua and Durham 2007) Conjunctivitis is also commonly associated to pollen-induced rhinitis.

Sensitization occurs at the site of allergen exposure, such as airways, but can also occur through the dermal tract. However, not everybody who is exposed will become sensitized and have allergies. Aside from the individual exposure conditions, there is a high variability in the individual responsiveness to a given allergen dose.

The most important allergen carriers in the outdoor air as well as in the indoor air are pollen – with a diameter between 15 and 60 mm – from anemophilic plants such as trees, grasses and weeds. In this thesis, we discuss five different species, which are Ambrosia, Artemisia, Betula, Gramineae and Quercus. However, whole pollen grains are too large to penetrate the small airways. Since pollen is able to evoke IgE-mediated allergic reactions within seconds after contact with the mucosa, pollen allergens must be extremely water soluble and readily available. In fact allergen liberation from pollen grains can occur on the mucosal surface of the upper respiratory tract after exposure to pollen(Behrendt and Becker 2001). Symptoms can be explained by the interaction between the antigen and its corresponding IgE antibody and this phase is situated at the end of a cascade of events leading to allergy. The experimental data

3.2 Pollen Season

Using different ways of observations and measurements, phenological events and pollen counts can be traced back to the same phenomenon, the flowering of plants.

Similarly, both kinds of data can in many respects be modeled with a similar set of observation-based models. Simple regression models can predict entry dates of phenological phases and likewise the start, peak and end of the pollen season or, given a greater number of independent variables, the day to day variability of the pollen counts. Phenological models will equally well predict the entry dates of phenological phases as well as the start, peak and end of the pollen season. Phenological models are sometimes grouped into the class of process-based models(Chuine, Belmonte et al. 2000), because they are built on assumptions rooted in experimental results on plant physiological responses to various environmental variables Methods

3.3 Data Collection

3.3.1. Pollen data Collection

Observed airborne pollen data from 85 monitor stations from 1994 to 2010 at nine different climates zones(Figure 3)in the US were studied to examine the annual mean and peak value of daily concentrations of five different species of pollens (Ambrosia, Artemisia, Betula, Gramineae, and Quercus). Time series Analysis were used to simulate start dates and season lengths of these five different kinds of pollen for the 17 year length data in contiguous US (CONUS). For most of the studied stations, comparison of mean pollen indices between the periods of 1994–2000 and 2001–2011 showed that these five different species pollen were observed to flower 1–3 weeks earlier; annual mean and peak value of daily pollen concentrations tended to increase by 10.6 %–248 %. The observed pollen season lengths varied for Ambrosia, Artemisia, Betula, Gramineae and Quercus across the different monitoring stations in the United States. Optimum initial date and base temperature for start date was found to be 25th July for Ambrosia [Figure 4]. The start data for Artemisia is 11th April [Figure 5], the start data for Betula is 29th March [Figure 6]. The start date for

Gramineae is 28th April [Figure 7] .the start date for Quercus is 22nd March [Figure 8].the pollen season lasts roughly 3months for each species, respectively. Simulation results indicated that responses of these different kinds of pollens to climate are expected to vary for different regions. Observed airborne pollen counts were obtained from monitoring stations of the American Academy of Allergy Asthma and Immunology (AAAAI) located in 9 different climate regions. The reported pollen data were classified only at the level of genus. Species under genus of Ambrosia, Artemisia, Betula, Gramineae or Quercus were not differentiated. Data used here are from March to September, which covers all the pollen season for all kinds of pollen species discussed above, the spatial distribution scenario of Betula in 2004 is displayed as an example, using VERDI. We are using logarithm instead of linear to make the figure clearer

3.3.2. Population data and Exposure Factor

The population data is from the United States census bureau. The demographic data contains the general population information(U.S 2010) ,in which the state-level population is by age group and sex. We combine those data, using ArcGIS to generate the population data on age and sex in 9 different climate regions to fit the corresponding pollen data.

The Exposure Factor data was obtained from EPA handbook(Agency 2010).those factor contains the value of inhalation ,dermal contact frequency ,skin surface, hand surface, indoor time/out time and other exposure factor data in different age groups and sex. In each age group, ten different percentiles level (0%-95%) and mean values of exposure factors are used to generate the exposure scenario in the nine climate zones.

These exposure factor data are all in country-level. a basic assumption is that the inhalation rate of the residents, as well as other exposure data, in different climate regions is identical, although the temperature ,illumination time and other environmental factors may surely affect those values.

3.4 Exposure Method Selection

3.3.3. Inhalation

Exposure can be quantified by multiplying the concentration of an agent times the duration of the contact. Exposure can be instantaneous when the contact between an agent and a target occurs at a single point in time and space .The summation of instantaneous exposures over the exposure duration is called the time-integrated exposure. Equation shows the time-integrated exposure(Fogh and Andersson 2000).

a) $$E = \int_{t1}^{t2} C(t)\,\mathrm{Idt} \tag{3.1}$$

where:

1. E = Time-integrated exposure (mass/volume),
2. t2– t1 = Exposure duration (ED) (time),
3. C = Exposure concentration as a function of time (mass/volume).
4. I = Inhalation factors(volume/time).

Dividing the time-integrated exposure by the exposure duration, results in the time-averaged exposure

In this article, since the time step is 1 day, we integrated the concentration through the whole pollen season (an average time about 3 months)for each species ,and we use pollen counts which is considered as a more appropriate measurement of the scenario..

Then we consider the indoor and outdoor scenario.

Outdoor:

$$E = \int_{t1}^{t2} C(t)\,\mathrm{Idt} \tag{3.2}$$

Indoor

$$E = \frac{\lambda_v}{\lambda_v + \lambda_d} \int_{t1}^{t2} C(t)\,\mathrm{Idt} \tag{3.3}$$

1. Where E = Time-integrated exposure (mass/volume),
2. t2– t1 = Exposure duration (ED) (time),
3. C = Exposure concentration as a function of time (mass/volume).
4. I = Inhalation factors (volume/time).
5. λ_d λ_v are ventilation rate and indoor deposition velocity, respectively.

3.3.4. Dermal Exposure

Dermal exposure to volatile chemical compound is fully studied already(Hu, Zhang et al. 2011), however, the reports to the dermal exposure to pollen remains rare. We use dry deposition model to estimate the adherence of pollen to human skins.

The dry deposition model assumed that the transport of material to the surface is to be governed by three resistances in series: the aerodynamic resistance r_a

the quasi-laminar layer resistance r_b, and the surface or canopy resistance r_c.The total resistance,r_t by definition, the inverse of the deposition velocity

$$v_d^{-1} = r_a + r_b + r_c \tag{3.4}$$

For particle dry deposition,v_d becomes

$$v_d = v_s + \frac{1}{r_a + r_b + r_a * r_b * v_s} \tag{3.5}$$

While v_s is the particle settling velocity

$$r_a = \frac{1}{ku_*}\ln\left(\frac{z}{z_0}\right) \tag{3.6}$$

$$r_b = 1/(u_*\left(Sc^{-\frac{2}{3}} + 10^{-\frac{3}{St}}\right) \tag{3.7}$$

$$v_s = \frac{\rho_p D_p^2 g C_c}{18\mu} \tag{3.8}$$

$$C_c = 1 + \frac{2\lambda}{D_p}\left(1.257 + 0.4e^{-\frac{0.55Dp}{\lambda}}\right) \tag{3.9}$$

Where ρ_p is the density of the particle, D_p is the particle diameter, g is the gravitational acceleration, μ is the viscosity of air, and C_c is the slip correction factor.

$$Sc = \frac{\mu}{\rho_a D} \tag{3.10}$$

$$St = \frac{v_s u_*^2 \rho_a}{g\mu} \tag{3.11}$$

$$D = \frac{k_B T C_C}{3\pi\mu D_p} \tag{3.12}$$

Where Sc is the Schmidt number, St is the Stokes number, and D is the molecular diffusivity,

So the direct deposition to the skin can be calculated now

1 indoor

$$M_{su} = A_{skin} v_d \int C(t)dt \tag{3.13}$$

2 outdoor

$$M_{su} = \frac{A_{skin} v_d \lambda_v}{\lambda_v + \lambda_d} \int C(t)dt \tag{3.14}$$

Where

1. $M_{su}$the mass of the substance in the skin surface
2. A_{skin} is the exposed skin area.
3. The parameters λ_d λ_v are ventilation rate and indoor deposition velocity, respectively.

3.5 Sensitivity Analysis Method Selection

Sensitivity analysis is the analysis of how the uncertainty in the output of a mathematical system or modeling(numerical or otherwise) can be apportioned to variety sources of uncertainty in its inputs.[1] A similar test is uncertainty analysis, which mainly focus on uncertainty quantification and propagation of uncertainty

Mean daily mass intake exposure to pollens was selected as a metric for testing the system's senility to multiple inputs and parameters. Global sensitivity analysis was performed based on Morris's Design. This design estimate the main

effect of a parameter by computing a number of local sensitivities at random points of the parameter space. The mean of these randomized local sensitivities indicates the overall influence of a given parameter on the output metric, while the corresponding standard deviation indication the effects of interacting and nonlinearity.

In the current study, each of the 17 parameters(Table 1) was sampled 3600 times according to the Morris method from 200 trajectories (each has 18 steps) in the parameter space. Each of the parameters in the simulation was perturbed from 50% to 150% of its base value or its distribution while we keep other parameters unchanged in the same time.

The mean daily exposure for sensitivity analyses was normally generated using 10000 “virtual men” in each climate regions in the flowering season. Equation was used to calculate the Normalized Sensitivity Coefficients(NSC) at a local point.

$$NSC_{i,j} = \frac{\frac{\Delta r_{ij}}{r_{ij}}}{\frac{\Delta p}{p}} \tag{3.15}$$

In this equation, the NSCi,j is the NSC for different exposure route i (inhalation, ingestion, dermal) in different climate regions j. the p is the input parameter values matrix, and r is the corresponding daily mean output of the exposure effect. The Δr and Δp is the corresponding perturbation of the parameter values and perturbation of the output, respectively. The global NSC of certain parameter, NSCg could be defined as the mean of the corresponding local sensitivities. We obtained the mean $\overline{\mathrm{NSCg}}$ for each route and scenario by averaging the NSC values on each trajectory. The standard deviations, in a similar way , are average over each exposure path and different climate regions scenarios. Then these values could be used to

evaluate the interaction and nonlinearity effect of input parameters on modeling output

3.6 Statistics of Concentrations, Exposure and Sensitivity Analysis

To generated statistics of concentrations, surface loading, exposures and sensitivity analysis, simulations were conducted using 100000 ”virtual residents” in these 9 different climate regions. Each resident will experience the whole flowering season with 5 kinds of pollens in different scenario (outdoor and indoor).

4 Result and Discussion

The exposure duration t can be set to different values for assessing exposure associated with different time durations. For example, it can be set to 1 hour to 24 hour to asses hourly to daily exposures.

Pesticide Concentration and Surface Loading. Figure 2 summarizes the statistics of 16 simulated pesticide air concentrations and surface loadings. The percentiles of boxplots were 17 calculated based on simulated surface loadings and concentrations averaged over 70 round trips 18 for each of the 100 “virtual aircraft cabins”. Residual Application tended to cause a higher 19 pesticide surface loading on the floor; its median was 2.1 and 9.5 times higher than those under 20 scenarios of Preflight spray and Top-of-Descent spray, respectively. This resulted partly from the 21 assumption that pyrethroid was an inertial species, which did not decompose on surfaces inside 22 aircraft cabins. Preflight spray tended to have a higher air

concentration with its median being

Sensitivity Analyses. The global sensitivity of the simulated exposures to different parameters

18 is illustrated in Figure 4. Overall, the global NSC of all parameters varied between -0.5 and 0.5, 19 indicating the robustness of the modeling approach. Ingestion and dermal exposures were more 20 sensitive to parameter perturbations, with average absolute global NSC, | NSCg | , being 0.15 and 21 0.11, respectively. Sensitive parameters included: single-touch transfer efficiency (TESHi), 22 deposition rate coefficient (kd), body weight (BW), portion of hand surface touching mouth (PH),

23 ratio of body surface to weight (FBS) and skin adhere efficiency (TEDS). Inhalation exposure was

The following figures are the simulated cumulative probability distributions of daily exposures of populations in the 9 nine climates regions to the 5 different kinds of pollens(Ambrosia,Artemisia,Betula,Gramineae,Quercus,respective

5 Conclusion

The modeling system developed based on physical processes and human activity data in the current study, can be easily adapted to simulated risks and exposure to particulate matter(PM) in similar environments or small scaled units such as cities or certain census. Furthermore, sensitivity analyses of the modeling system provides helpful information for planning measurements related to investigation of health risks associated with occupational exposures to pollens or other kinds or particulate particles in the environments.

6 Figure

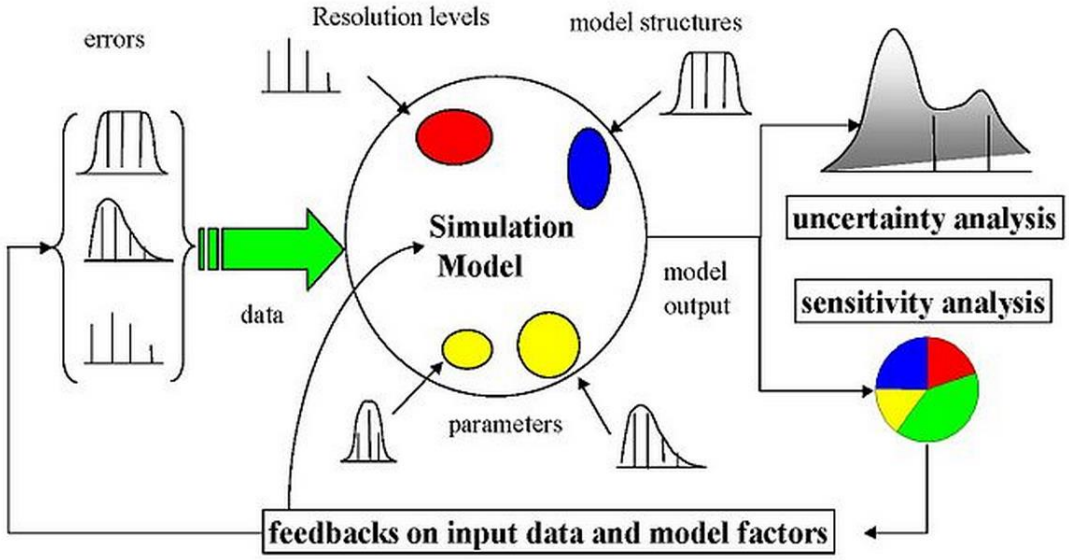

Figure 1 Scheme for sensitivity anaylsis

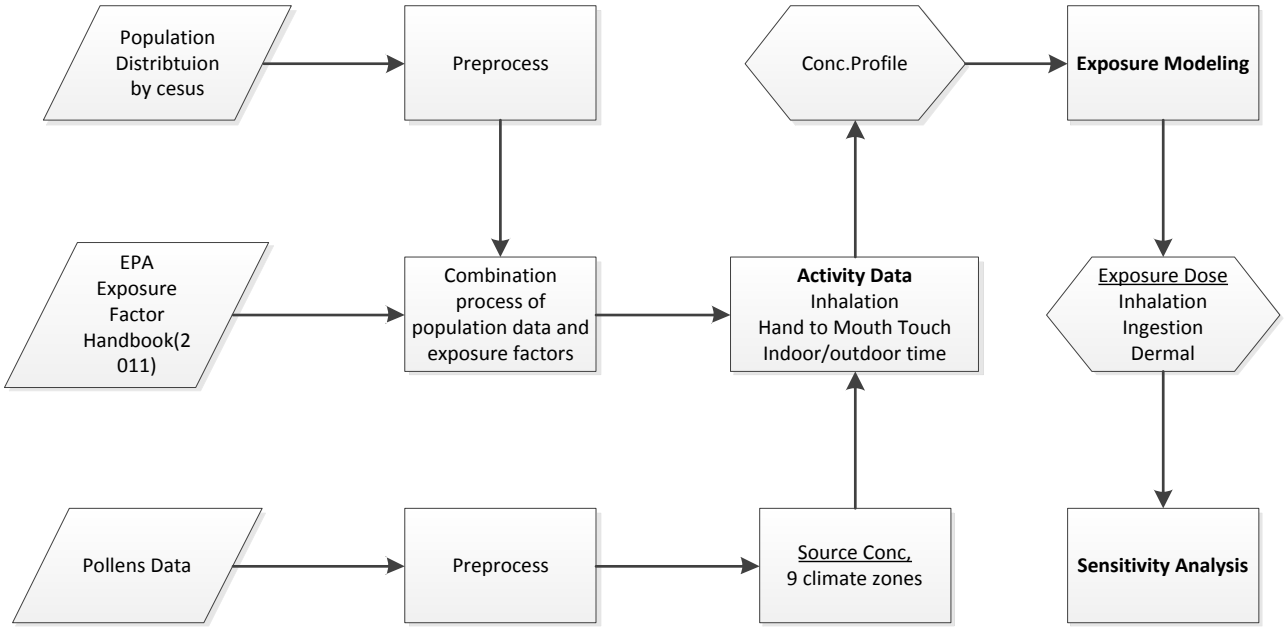

Figure 2 Schematic diagram of modeling occupational exposure of population exposure to pollens in 9 climate regions. Concentrations and surface loading of pollens were simulated based on mass balance and source concentrations from fluid dynamic model. Exposures to pollens were simulated based on the concentration profiles and activity data of different groups by ages and sex from United States Census Bureau. The intake dosed calculated from exposure modeling are then used as input to conduct sensitivity analysis.

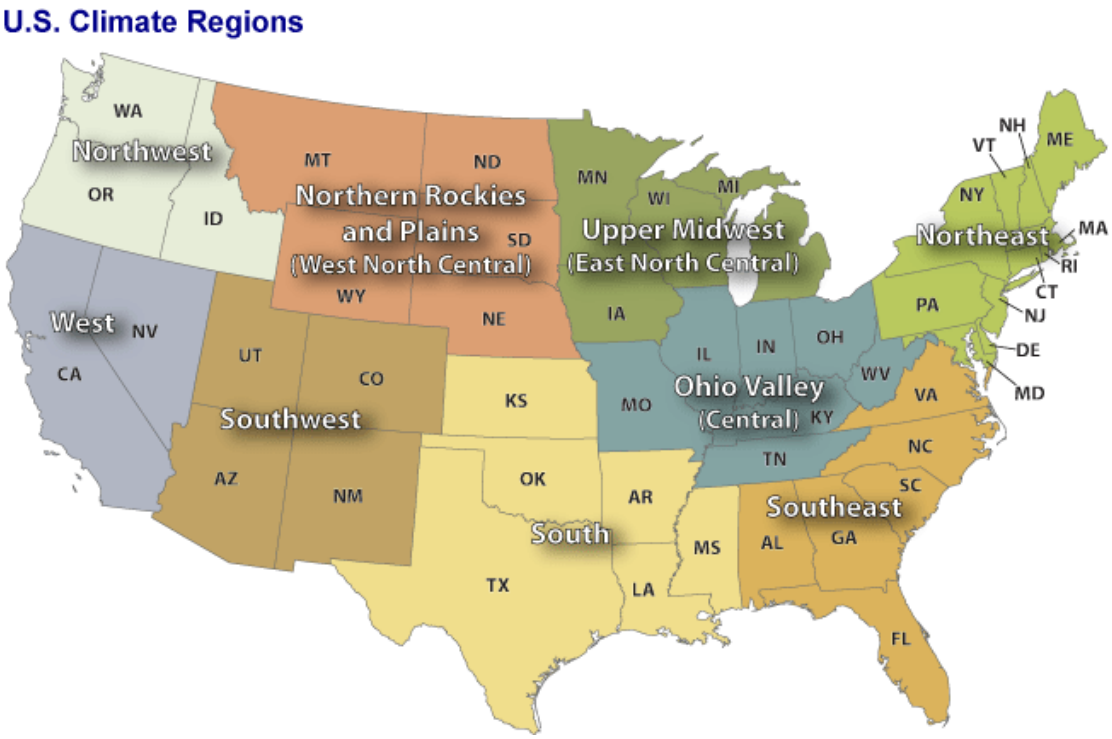

Figure 3 Through climate analysis, National Climatic Data Center scientists have identified nine climatically consistent regions within the contiguous United States which are useful for putting current climate anomalies into a historical perspective(Karl and Koss 1984)

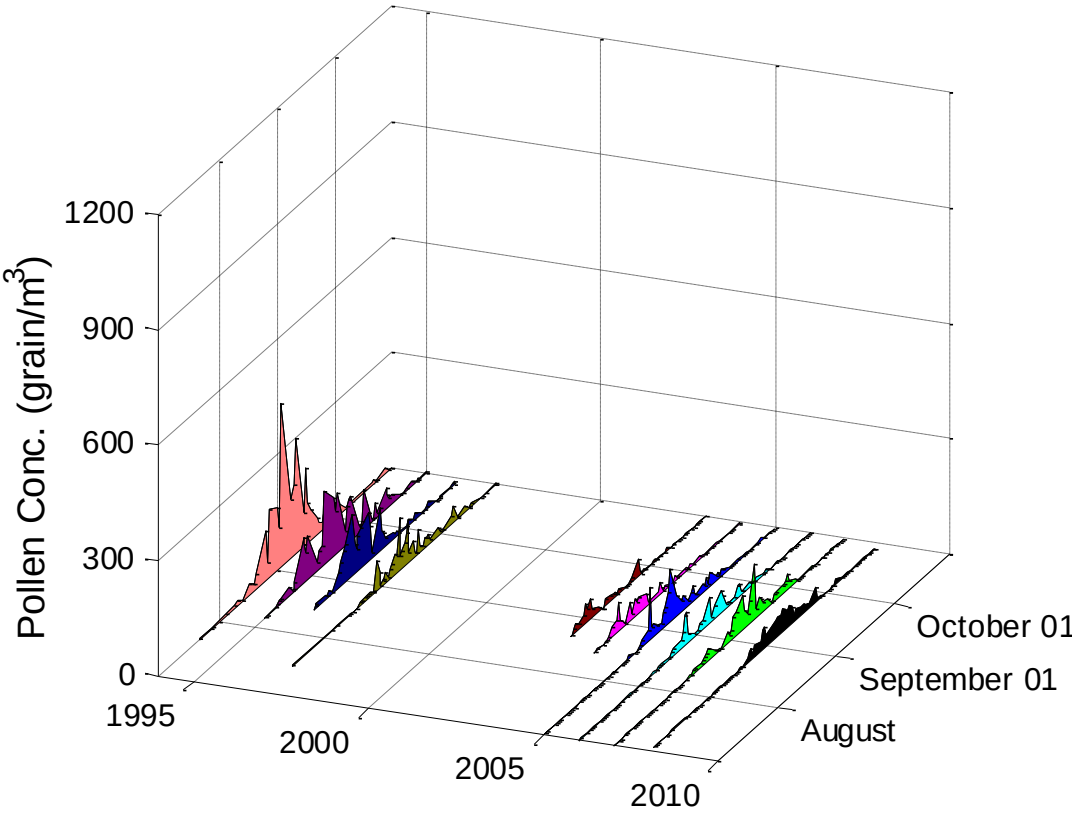

Figure 4 time series analysis of pollen concentration of Ambrosia in UMDNJ monitor station which located in the Northeast Climate Zones. The pollen data is from National Allergy Bureau(Bureau 2010).we can see clearly that the start date of Ambrosia is July 25th.the flowering season lasts about 3 months.

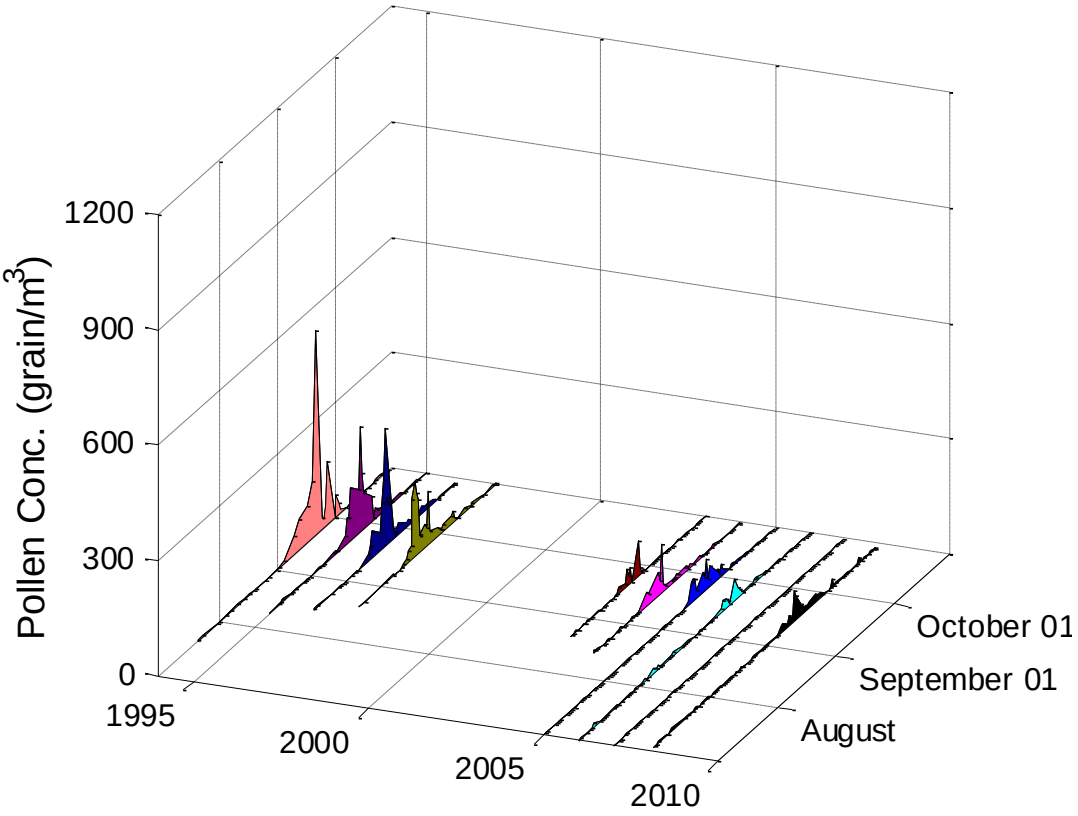

Figure 5 time series analysis of pollen concentration of Artemisia in UMDNJ monitor station which located in the Northeast Climate Zones. The pollen data is from National Allergy Bureau(Bureau 2010) we can see clearly that the start date of Artemisia is August 11th.the flowering season lasts about 3 months. The peak value appear from early September to ear October.

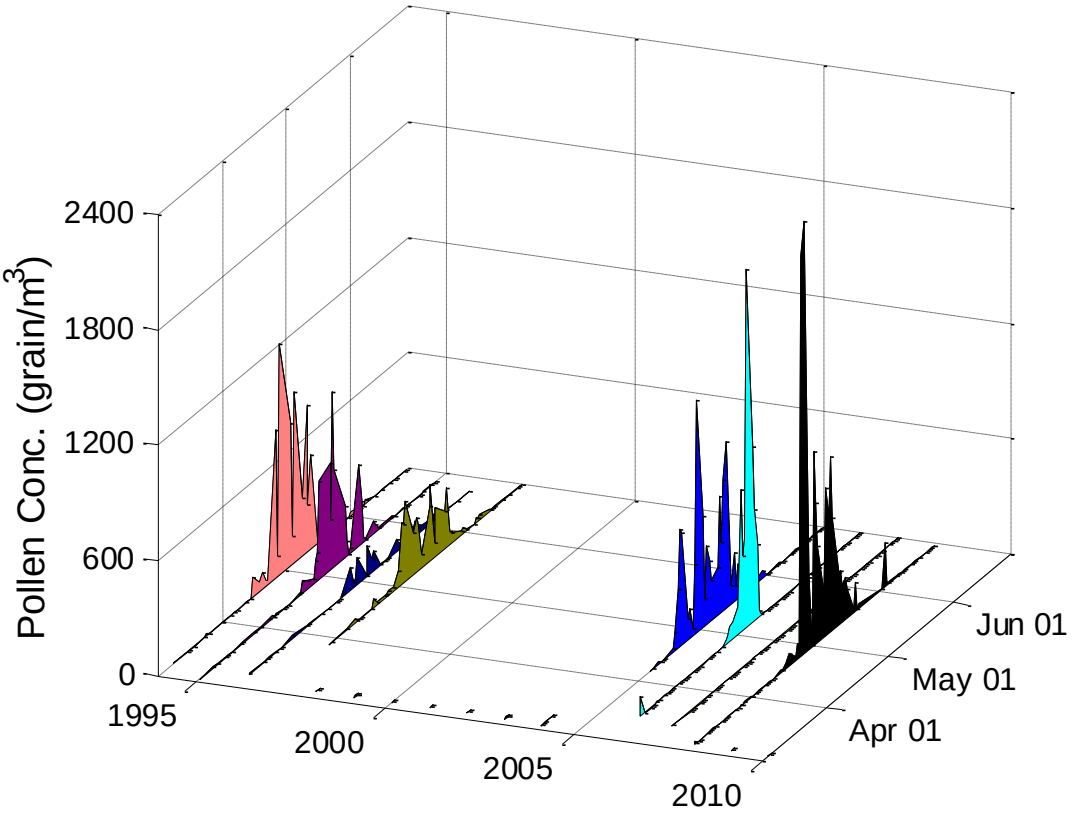

Figure 6 time series analysis of pollen concentration of Betula in UMDNJ monitor station which located in the Northeast Climate Zones. The pollen data is from National Allergy Bureau(Bureau 2010). We can see clearly that the start date of Betula is March 29th.the flowering season lasts about 3 months. The peak value appear from middle of the April to last May.

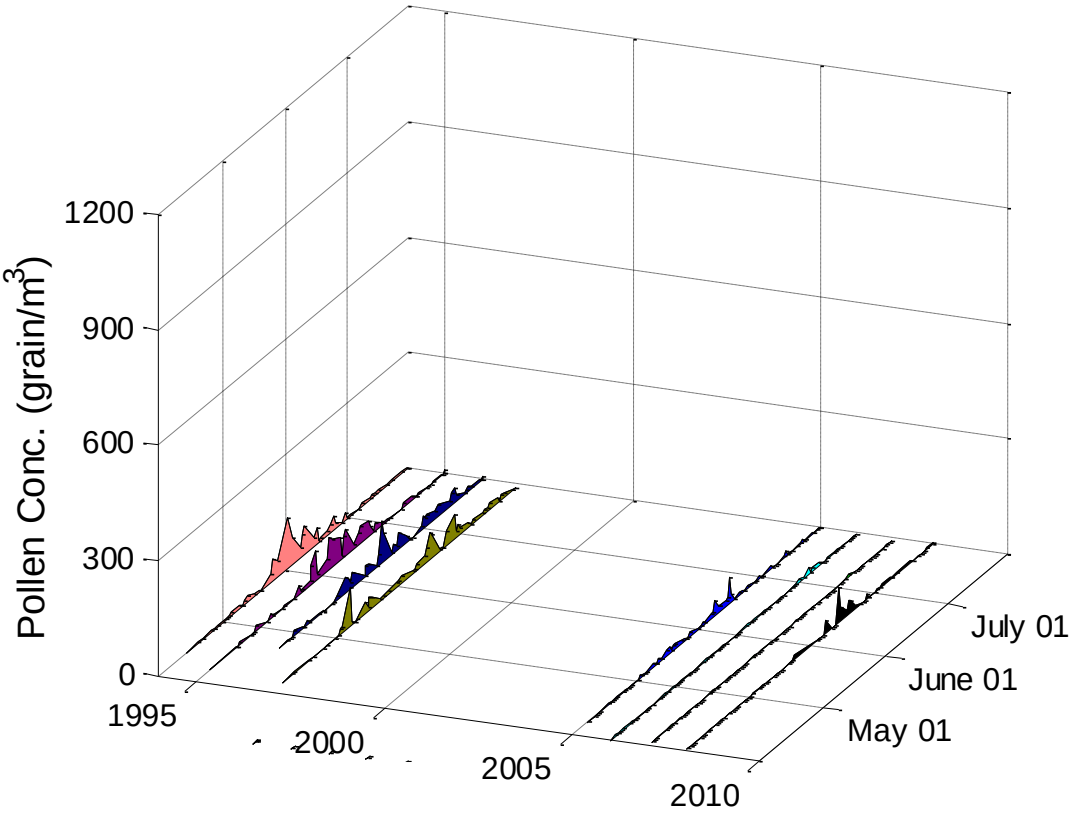

Figure 7 time series analysis of pollen concentration of Gramineae in UMDNJ monitor station which located in the Northeast Climate Zones. The pollen data is from National Allergy Bureau(Bureau 2010). We can see clearly that the start date of Gramineae is April 28th.the flowering season lasts about 3 months. The peak values appear from last May to early June

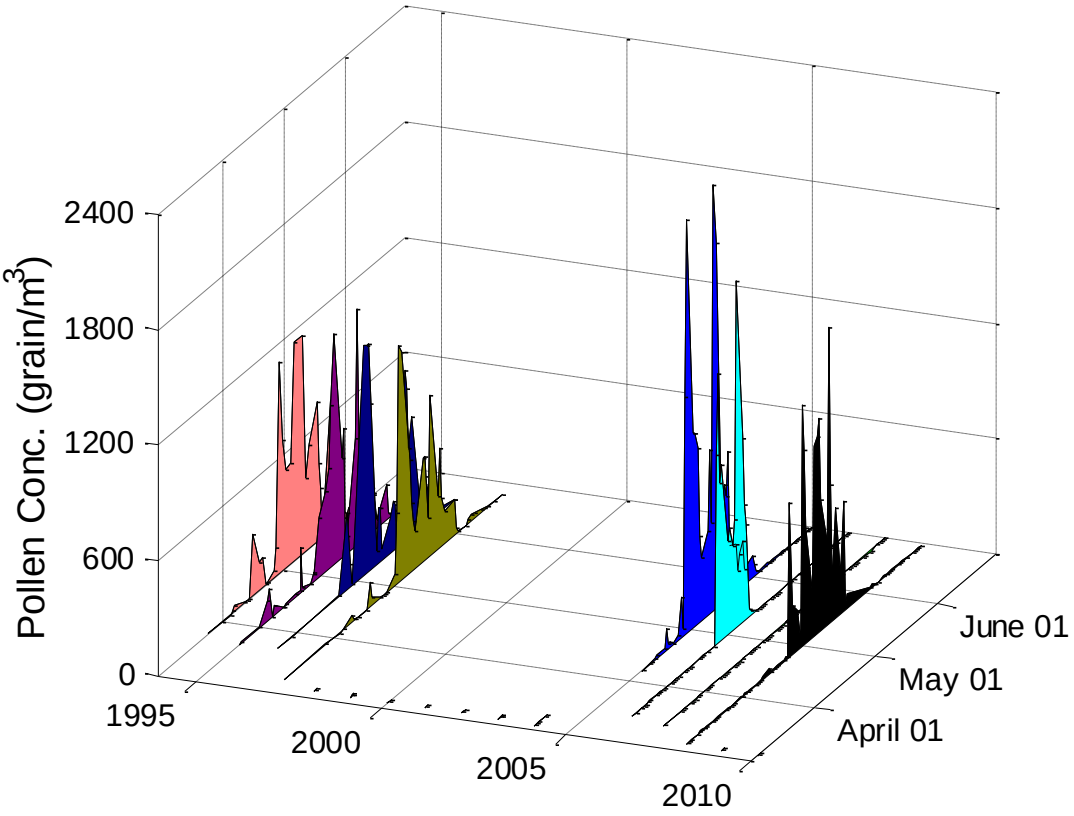

Figure 8 Quercus time series analysis of pollen concentration of Ambrosia in UMDNJ monitor station which located in the Northeast Climate Zones. The pollen data is from National Allergy Bureau(Bureau 2010) We can see clearly that the start date of Quercus is March 22th.the flowering season lasts about 3 months. The peak values appear from late April to early June.

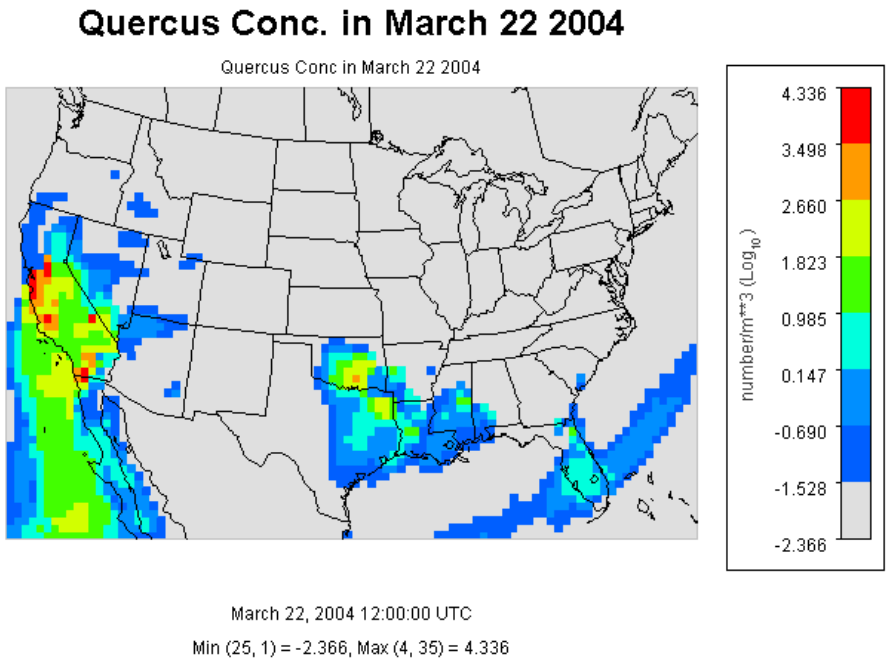

Figure 9 Quercus Concentration in 2004.the scenario is in 11:00am March 22,which is considered as the start data of the pollen season. We can see that in southwest coast ,there is already some pollens exists, but the concentration is very low. in other parts of the states, there remains few pollens.

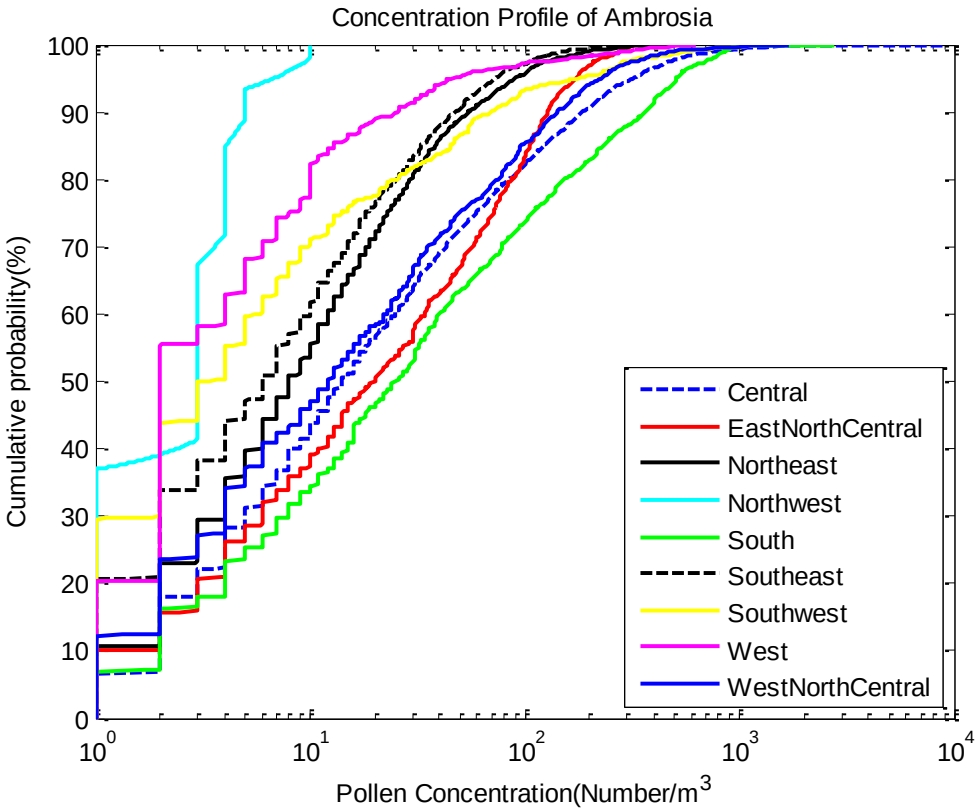

Figure 10 the simulated cumulative probability distributions of Ambrosia's pollen concentration of populations in the 9 nine climates regions.

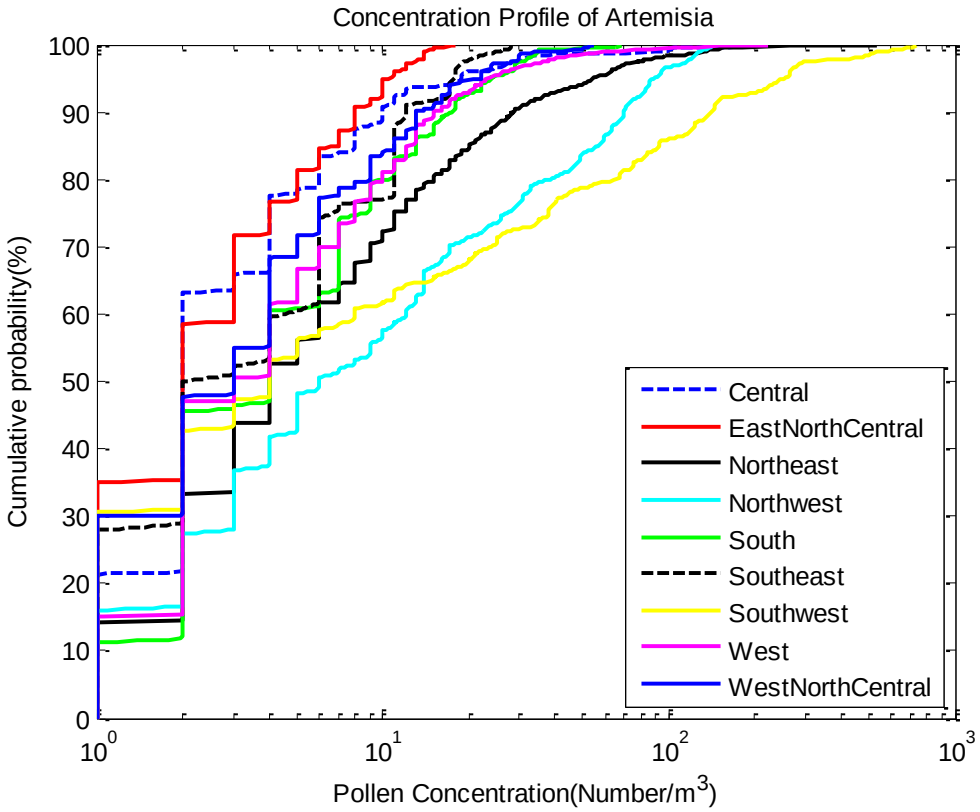

Figure 11 the simulated cumulative probability distributions of Artemesisa's pollen concentration of populations in the 9 climates regions.the concentration profile in southwest is slightly smooth than in other climate regions

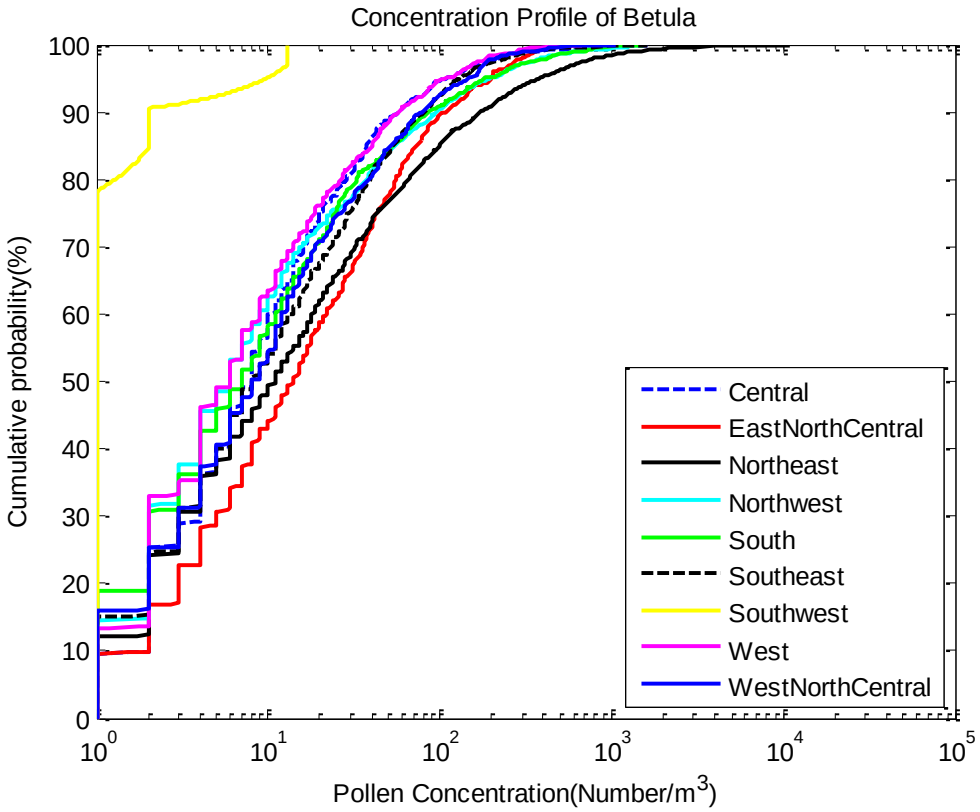

Figure 12 the simulated cumulative probability distributions of Betula's pollen concentration of populations in the 9 climates regions.

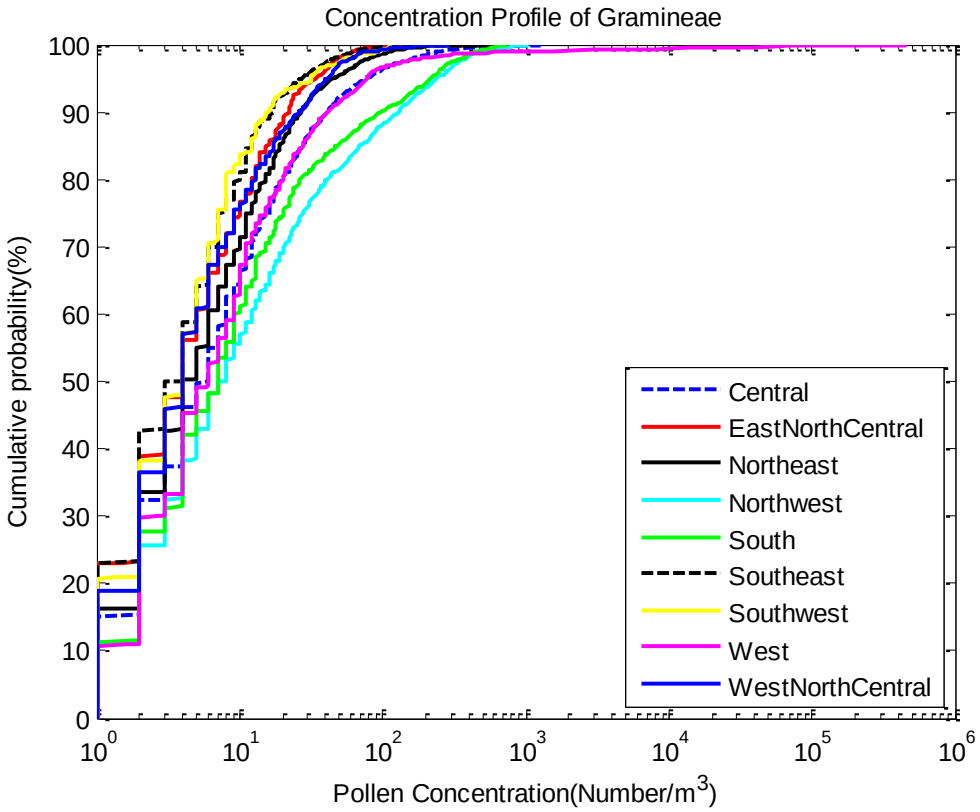

Figure 13 the simulated cumulative probability distributions of Gramineae's pollen concentration of populations in the 9 climates regions.

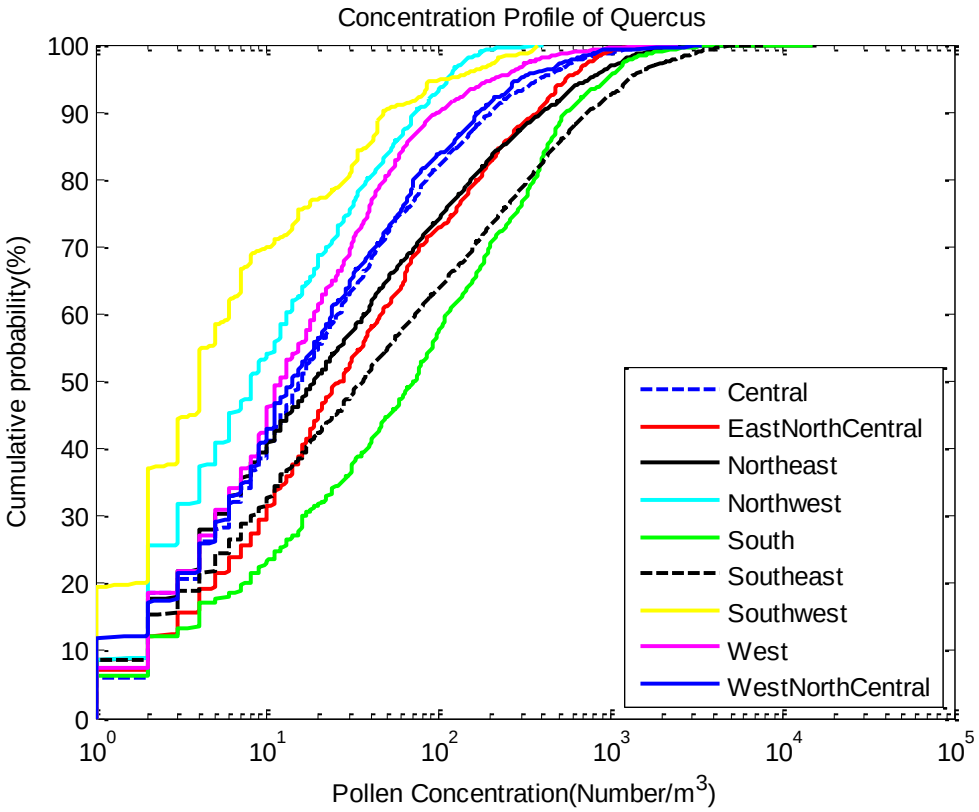

Figure 14 the simulated cumulative probability distributions of Quercus' pollen concentration of populations in the 9 climates regions.

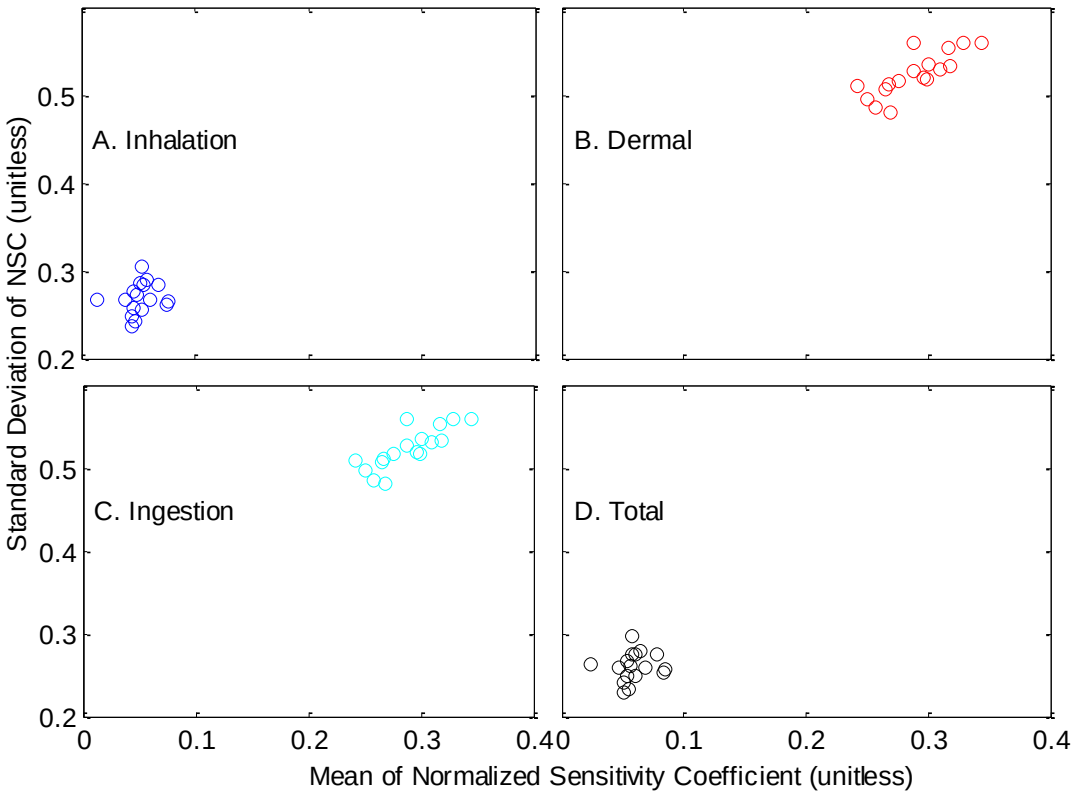

Figure 15 Mean and Standard Deviation of Normalized Sensitivity Coefficient(NSC) for population exposure in the united states(9 regions combined data) (A) Inhalation (B)Dermal (C) Ingestion (D)Total Exposures

7 Table

Station ID	Station Name	Lat (N)	Lon (W)	Elevation	Climate Region
3	Corpus Christi, TX	27.8	97.4	2.00	South
4	Tampa, FL	28.06	82.43	12.00	Southeast
9	Tallahassee, FL	30.44	84.28	62.00	Southeast
10	Georgetown, TX	30.64	96.31	91.00	South
11	College Station, TX	30.64	97.76	269.00	South
12	Waco, TX	31.51	97.2	185.00	South
17	Dallas, TX	33.04	96.83	207.00	South
19	Scottsdale, AZ	33.49	111.92	377.00	Southwest
21	Orange, CA	33.78	117.86	53.00	West
22	Atlanta, GA	33.97	84.55	366.00	Southeast
24	Santa Barbara, CA	34.44	119.76	57.00	West
25	Huntsville, AL	34.73	86.59	191.00	Southeast
26	Little Rock, AR	34.75	92.39	115.00	South
28	Charlotte, NC	35.3	80.75	229.00	Southeast
29	Fort Smith, AR	35.35	94.39	186.00	South
30	Oklahoma City, OK	35.61	97.6	340.00	South
31	Los Alamos, NM	35.88	106.32	2227.00	Southwest
32	Knoxville, TN	35.95	84.01	305.00	Central
33	Tulsa 1, OK	36.03	95.87	207.00	South
34	Durham, NC	36.05	78.9	110.00	Southeast
35	Las Vegas, NV	36.17	115.15	620.00	West
38	San Jose 2, CA	37.31	121.97	47.00	West
39	San Jose 2, CA	37.33	121.94	35.00	West
40	Pleasanton, CA	37.69	121.91	100.00	West
42	Lexington, KY	38.04	84.5	299.00	Central
43	Roseville, CA	38.76	121.27	57.00	West
44	Colorado Springs 2, CO	38.87	104.82	1867.00	Southwest
45	Colorado Springs 1, CO	38.87	104.83	1868.00	Southwest
46	Kansas City, MO	39.08	94.58	288.00	Central
47	Baltimore, MD	39.37	76.47	36.00	Northeast
48	Reno, NV	39.56	119.77	1382.00	West
49	New Castle, DE	39.66	75.57	3.00	Northeast
50	Indianapolis, IN	39.91	86.2	254.00	Central

Table 1 Through climate analysis, National Climatic Data Center scientists have identified nine climatically consistent regions within the contiguous United States which are useful for putting current climate anomalies into a historical perspective(Karl and Koss 1984)

Station ID	Station Name	Lat (N)	Lon (W)	Elevation	Climate Region
51	York, PA	39.94	74.91	13.00	Northeast
52	Cherry Hill, NJ	39.94	76.71	195.00	Northeast
53	Philadelphia, PA	39.96	75.16	12.00	Northeast
54	Pittsburgh, PA	40.47	79.95	287.00	Northeast
58	Newark, NJ	40.74	74.19	43.00	Northeast
59	Lincoln, NE	40.82	96.64	371.00	West North Central
60	Armonk, NY	41.13	73.73	187.00	Northeast
61	Omaha, NE	41.14	95.97	305.00	West North Central
62	Waterbury, CT	41.55	73.07	140.00	Northeast
64	Chicago, IL	41.91	87.77	189.00	Central
65	Olean, NY	42.09	78.43	433.00	Northeast
66	Erie, PA	42.1	80.13	215.00	Northeast
67	Salem, MA	42.5	70.92	42.00	Northeast
68	St. Clair Shores, MI	42.51	82.9	180.00	East North Central
69	Twin Falls, ID	42.58	114.46	1124.00	Northwest
70	Chelmsford, MA	42.6	71.35	37.00	Northeast
71	Albany, NY	42.68	73.77	72.00	Northeast
72	London, ON, Canada	42.99	81.25	250.00	Central
73	Waukesha, WI	43.02	88.24	270.00	East North Central
74	Madison, WI	43.08	89.43	263.00	East North Central
75	Niagara Falls, ON , Canada	43.09	79.09	188.00	Northeast
76	Rochester, NY	43.1	77.58	148.00	Northeast
78	LaCrosse, WI	43.88	91.19	216.00	East North Central
79	Eugene, OR	44.04	123.09	129.00	Northwest
81	Vancouver, WA	45.62	122.5	89.00	Northwest
83	Fargo, ND	46.84	96.87	277.00	West North Central
85	Seattle, WA	47.66	122.29	20.00	Northwest

Table 2 Through climate analysis, National Climatic Data Center scientists have identified nine climatically consistent regions within the contiguous United States which are useful for putting current climate anomalies into a historical perspective(Karl and Koss 1984)

parameter1	Parameter	ID	Distribution	Mean(STD)
ustar	friction velocity(m/s)	1	fixed	1.17
k	von karman constant(dimensionless)	2	fixed	0.41
Dp	diameter of pollen(m)	3	fixed	2.00E-05
Pp	density of pollen(kg/m3)	4	fixed	840
mu	viscosity of air (m/s)	5	fixed	1.81E-05
namda	mean free path of air molecules(m)	6	fixed	6.80E-08
pa	density of air(kg/m3)	7	fixed	1.145
T	temperature(k)	8	range	298
Ve	ventilation rate(dimensionless)	9	range	1.2
indtime	indoor time(min)	10	norm	1279(21)
outtime	outdoor time(min)	11	norm	174(4)
derm	hand to mouth contact frequency	12	empirical	30
Sa	human surface area(m2)	13	lognorm	1.76
Sr	hand surface rate(%)	14	lognorm	5.3
Ihf	female inhalation rate (m3/day)	15	uniform	1.33
Ihm	male inhalation rate(m3/day)	16	uniform	1.45
Vd	indoor velidation rate(dimensionless)	17	empirical	1.75

Table 3 Parameters for calculating population exposure to pollens in 9 different climate regions in United States.These parameters were listed either as fixed valueds,known distribtuons or unkown empirical distribution derived from the literatures.

8 Reference

Adhikari, A., et al. (2006). "Correlation of ambient inhalable bioaerosols with particulate matter and ozone: a two-year study." Environmental Pollution **140**(1): 16-28.

Agency, U. E. P. (2010). Exposure factors handbook, EPA Washington, DC.

Bateman, E., et al. (2008). "Global strategy for asthma management and prevention: GINA executive summary." European Respiratory Journal **31**(1): 143-178.

Beamer, P., et al. (2008). "Developing probability distributions for transfer efficiencies for dermal exposure." Journal of Exposure Science and Environmental Epidemiology **19**(3): 274-283.

Behrendt, H. and W.-M. Becker (2001). "Localization, release and bioavailability of pollen allergens: the influence of environmental factors." Current Opinion in Immunology **13**(6): 709-715.

Bielory, L., et al. (2012). "Climate change and allergic disease." Current allergy and asthma reports **12**(6): 485-494.

Bousquet, J., et al. (2008). "Allergic rhinitis and its impact on asthma (ARIA) 2008*." Allergy **63**(s86): 8-160.

Brożek, J. L., et al. (2010). "Allergic Rhinitis and its Impact on Asthma (ARIA) guidelines: 2010 revision." Journal of Allergy and Clinical Immunology **126**(3): 466-476.

Bureau, N. A. (2010). NAB Pollen Counts.

Bureau, U. S. C. (2010). Profile of General Population and Housing Characteristics: 2010 Census Summary File.

Chuine, I., et al. (2000). "A modelling analysis of the genetic variation of phenology between tree populations." Journal of Ecology **88**(4): 561-570.

Damialis, A., et al. (2007). "Long-term trends in atmospheric pollen levels in the city of Thessaloniki, Greece." Atmospheric Environment **41**(33): 7011-7021.

Eder, W., et al. (2006). "The asthma epidemic." New England Journal of Medicine **355**(21): 2226-2235.

Fogh, C. L. and K. G. Andersson (2000). "Modelling of skin exposure from distributed sources." Annals of Occupational Hygiene **44**(7): 529-532.

Hu, X., et al. (2011). "Bioaccessibility and health risk of arsenic, mercury and other metals in urban street dusts from a mega-city, Nanjing, China." Environmental Pollution **159**(5): 1215-1221.

Karl, T. and W. J. Koss (1984). Regional and National Monthly, Seasonal, and Annual Temperature Weighted by Area, 1895-1983, National Climatic Data Center.

Lamb, C. E., et al. (2006). "Economic impact of workplace productivity losses due to allergic rhinitis compared with select medical conditions in the United States from an employer perspective." Current Medical Research and Opinion® **22**(6): 1203-1210.

Obtułowicz, K. (1992). "Air pollution and pollen allergy." Folia Medica Cracoviensia **34**(1-4): 121-128.

Passalacqua, G. and S. R. Durham (2007). "Allergic rhinitis and its impact on asthma update: allergen immunotherapy." Journal of Allergy and Clinical Immunology **119**(4): 881-891.

Saltelli, A., et al. (2000). Sensitivity analysis, Wiley New York.

Shea, K. M., et al. (2008). "Climate change and allergic disease." Journal of Allergy and Clinical Immunology **122**(3): 443-453.

Singh, K., et al. (2010). "The epidemiology of ocular and nasal allergy in the United States, 1988-1994." Journal of Allergy and Clinical Immunology **126**(4): 778-783. e776.

Sofiev, M., et al. (2013). Airborne Pollen Transport. Allergenic Pollen, Springer**:** 127-159.

U.S, C. B. (2010). "Profile of General Population and Housing Characteristics: 2010 more information

2010 Census File."

Zhang, Y., et al. (2013). "Climate change effect on Betula (birch) and Quercus (oak) pollen seasons in the United States." International Journal of Biometeorology: 1-11.

Zhang, Y., et al. (2013). "Bayesian analysis of climate change effects on observed and projected airborne levels of birch pollen." Atmospheric Environment **68**(0): 64-73.